

## COGNITIVE NEUROSCIENCE

# Prediction of memory formation based on absolute electroencephalographic phases in rhinal cortex and hippocampus outperforms prediction based on stimulus-related phase shifts

Marlene Derner,<sup>1</sup>  Amirhossein Jahanbekam,<sup>1</sup> Christian Bauckhage,<sup>2,3</sup> Nikolai Axmacher<sup>4</sup> and Juergen Fell<sup>1</sup><sup>1</sup>Department of Epileptology, University of Bonn, Sigmund-Freud-Str. 25, D-53105 Bonn, Germany<sup>2</sup>Bonn-Aachen International Center for Information Technology, University of Bonn, Bonn, Germany<sup>3</sup>Fraunhofer Institute for Intelligent Analysis and Information Systems IAIS, Sankt Augustin, Germany<sup>4</sup>Department of Neuropsychology, Institute of Cognitive Neuroscience, Faculty of Psychology, Ruhr University Bochum, Bochum, Germany**Keywords:** intracranial EEG, long-term memory, machine learning, phase, prediction

## Abstract

Absolute (i.e. measured) rhinal and hippocampal phase values are predictive for memory formation. It has been an open question, whether the capability of mediotemporal structures to react to stimulus presentation with phase shifts may be similarly indicative of successful memory formation. We analysed data from 27 epilepsy patients implanted with depth electrodes in the hippocampus and entorhinal cortex, who performed a continuous word recognition task. Electroencephalographic phase information related to the first presentation of repeatedly presented words was used for prediction of subsequent remembering vs. forgetting applying a support vector machine. The capability to predict successful memory formation based on stimulus-related phase shifts was compared to that based on absolute phase values. Average hippocampal phase shifts were larger and rhinal phase shifts were more accumulated for later remembered compared to forgotten trials. Nevertheless, prediction based on absolute phase values clearly outperformed phase shifts and there was no significant increase in prediction accuracies when combining both measures. Our findings indicate that absolute rhinal and hippocampal phases and not stimulus-related phase shifts are most relevant for successful memory formation. Absolute phases possibly affect memory formation via influencing neural membrane potentials and thereby controlling the timing of neural firing.

## Introduction

Long-term memory (LTM) formation critically depends on neural operations within the rhinal cortex and hippocampus. Intracranial EEG (iEEG) recordings in presurgical epilepsy patients have revealed several rhinal and hippocampal EEG characteristics that are associated with successful memory encoding (e.g. Sederberg *et al.*, 2007; Fell *et al.*, 2008; Lopour *et al.*, 2013; Burke *et al.*, 2014). Hereby, rhinal and hippocampal EEG measures reflecting the stability of phases across trials, such as inter-trial phase locking and rhinal–hippocampal phase synchronisation, appear to be better suited to distinguish subsequently remembered from forgotten trials than event-related potentials or amplitude-based measures (Fell *et al.*,

2008; Lopour *et al.*, 2013). We hypothesised that increased inter-trial phase locking and phase synchronisation may be related to a higher occurrence of optimal phase values or phase differences. Via spike-field coupling, these optimal phase values or phase differences may facilitate neural firing and communication and thereby promote memory formation (e.g. Womelsdorf *et al.*, 2007; Fell & Axmacher, 2011).

Recently, we have found evidence for this hypothesis by evaluating whether single-trial rhinal and hippocampal phase values are predictive for successful memory formation (Höhne *et al.*, 2016). Applying machine learning techniques, for the majority of investigated subjects (23 of 27) above-chance prediction was possible based on only three single-trial phase values: one rhinal phase, one hippocampal phase and one rhinal–hippocampal phase difference. Average prediction accuracy based on the phase values was 69.2% and clearly outperformed predictions based on power values. However, it remained an open question whether absolute phases, that is the phases measured at certain time points, are indeed most crucial for memory formation.

**Correspondence:** Marlene Derner, as above. E-mail: marlene.derner@ukbonn.de

Received 15 August 2017, revised 31 January 2018, accepted 18 February 2018

Edited by Thomas Klausberger. Reviewed by Robert Knight, UC Berkeley, USA; and Frederic Roux, University of Birmingham, UK

All peer review communications can be found with the online version of the article.

Absolute phases derive from three different factors: the phase values at stimulus presentation, frequency-specific phase progressions and stimulus-related phase shifts. The phase progression results from the frequency considered and the time elapsed since stimulus presentation that is it determines the expected phase value in case no stimulus-related phase perturbation would occur. A deviation of the measured phase (absolute phase) from the expected value points to a stimulus-related phase shift. The capability of mediotemporal structures to react to stimulus presentation with phase shifts may be indicative of effective stimulus processing and may facilitate memory encoding (e.g. Achuthan & Canavier, 2009). Thus, we wondered whether the magnitude of rhinal and hippocampal phase shifts is related to successful memory formation and whether phase shifts are similarly well-suited to predict subsequent memory as absolute phases.

## Materials and methods

To answer these questions, we reanalysed EEG signals recorded from the hippocampus and rhinal cortex of 27 presurgical epilepsy patients (13 female, 20–61 years, mean age 40.6) while they performed a continuous word recognition task (see Höhne *et al.*, 2016). The ERP waveforms, power spectra and inter-trial phase locking findings for these data were reported in Fell *et al.* (2008). Each patient provided written informed consent. The study conformed to the World Medical Association Declaration of Helsinki 2013 and was approved by the local ethics committee of the Medical Faculty at the University of Bonn.

In brief, German nouns were presented, of which 150 were shown only once and the other 150 were presented with one repetition. Each word was presented for 300 ms with an individually adjusted inter-stimulus interval of 1600 ms, 2000 ms or  $2700 \pm 200$  ms.

Inter-stimulus intervals were adjusted based on each individual patient's performance over a few practice trials, which were conducted before the experiment. The individual adjustments aimed to enable patients to respond to each word using both response keys. Subjects had to decide whether they had previously seen the word before (old) or not (new). Responses to the first presentation were classified as subsequently 'remembered' or 'forgotten' depending on whether the word was correctly identified or not at the second presentation (Fig. 1A).

Electroencephalographic data were recorded using intracranial depth electrodes, which were bilaterally implanted along the longitudinal axis of the hippocampus. In a first step, electrode contact placement was ascertained by examining individual MRIs in comparison with standardised anatomical atlases (e.g. Duvernoy, 1988). Then, for each patient from the contacts localised within rhinal cortex, the contact with the largest mean negative amplitude (new words) in the time range between 200 and 600 ms (N400 component) was selected. From the contacts localised within the hippocampus, the contact with the largest mean amplitude (new words) in the time range between 300 and 1500 ms (P600 component) was selected (see also Ludwig *et al.*, 2008). Only contacts contralateral to the ictal onset zone were considered for analysis (Fig. 1B). Phase information in the encoding trials (first presentation of repeatedly presented words) was used for prediction of subsequent remembering vs. forgetting applying a linear support vector machine (SVM). Prediction accuracies based on stimulus-related phase shifts were compared with those based on absolute phase values.

The set of features to predict subsequent memory was given by one rhinal phase, one hippocampal phase and one rhinal–hippocampal phase difference. Phase values were extracted using a second-order two-pass Butterworth filter (bandwidth = 1 Hz; FieldTrip toolbox; Oostenveld *et al.*, 2011, for MATLAB Version 8.2; The

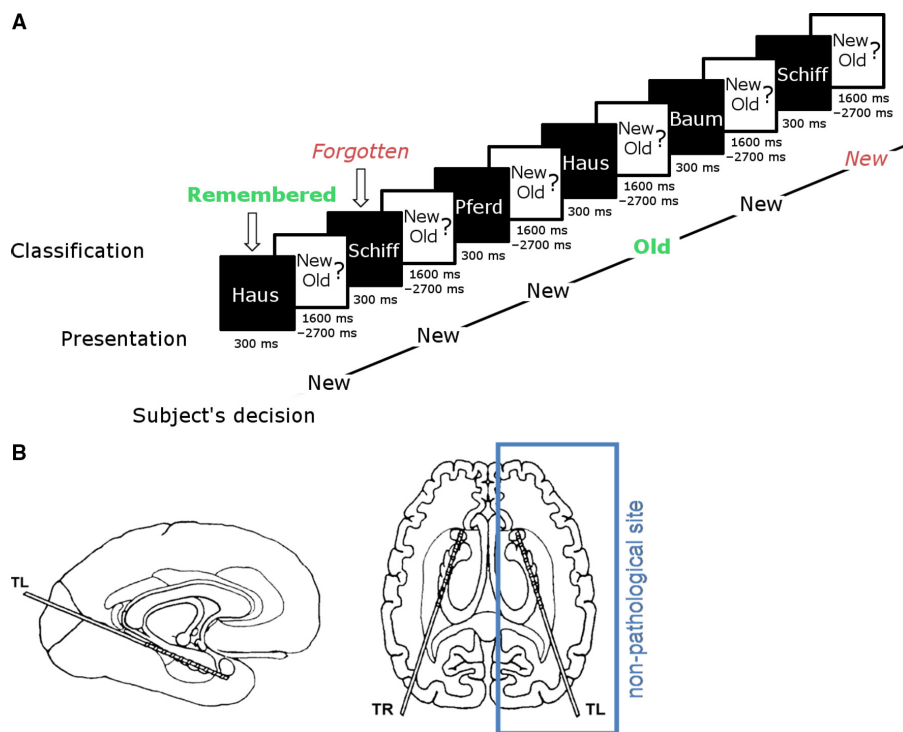


FIG. 1. (A) Continuous word recognition paradigm. Patients had to remember common German words and trials of the first presentation were classified into remembered or forgotten based on their response to the second presentation of a word. (B) Electrode implantation site. Only electrodes from the non-pathological site were considered for the analysis. [Colour figure can be viewed at [wileyonlinelibrary.com](http://wileyonlinelibrary.com)].

MathWorks Inc.) and Hilbert transformation. The relative phase  $\varphi_{\text{rel}}$  at a specific poststimulus time point  $t = \text{tx}$  is given by the difference between the absolute phase  $\varphi_{\text{abs}}$  at  $\text{tx}$  and the absolute phase  $\varphi_{\text{abs}}$  at stimulus onset ( $t = 0$  ms), that is  $\varphi_{\text{rel}}(\text{tx}) = \varphi_{\text{abs}}(\text{tx}) - \varphi_{\text{abs}}(0)$ . The relative phase  $\varphi_{\text{rel}}(\text{tx})$  can be deconstructed into two contributions: the progression  $2\pi f^* \text{tx}$  depending on the selected EEG frequency  $f$  and the time point  $\text{tx}$ , and the stimulus-related phase shift  $\Delta\varphi$ , that is  $\varphi_{\text{rel}}(\text{tx}) = 2\pi f^* \text{tx} + \Delta\varphi$ . Thus, for a given time point  $\text{tx}$  and frequency  $f$  the phase shift  $\Delta\varphi$  can be quantified as:  $\Delta\varphi = \varphi_{\text{rel}}(\text{tx}) - 2\pi f^* \text{tx}$ .

For SVM classification, frequencies from 0.5 to 50 Hz were considered (0.5 Hz steps). Features were selected from the poststimulus interval between 0 and 2000 ms (please note that features were also chosen from the prestimulus range in Hühne *et al.* (2016)). For each patient, a set of training (60%), validation (20%) and test trials (20%) was randomly chosen. One specific frequency and time point were selected for each patient and measure based on significant differences between the phases or phase shifts for the conditions ‘remembered’ and ‘forgotten’ in the training trials (circular Kruskal–Wallis test; CircStat toolbox for MATLAB; Berens, 2009). For each patient and each measure, the 10 time-frequency points showing the most significant differences between conditions (remembered vs. forgotten), based on the circular version of the Kruskal–Wallis test were preselected. Then, from these 10 time-frequency points, one final time-frequency point was selected for each patient and measure based on the highest prediction accuracies in the validation data. Based on these final time-frequency points, the absolute phases and phase shifts were determined as features for classification of the test data. Importantly, frequency and time points were independently selected for phases and phase shifts (see Table 1 and Fig. 2 for

distributions of frequencies and time points). These phases and phase shifts were deconstructed into their sine and cosine contributions and a support vector machine was trained to distinguish subsequently remembered from forgotten trials. This support vector machine was applied to new trials and classification accuracies were evaluated for each patient.

Above-chance significance of prediction accuracies was calculated for each subject based on non-parametric label permutation statistics (Maris & Oostenveld, 2007). For this purpose, trial labels (remembered/forgotten) were randomly shuffled 1000 times and then these surrogate trials were subjected to the same classification procedure as the original trials. The statistical significance of above-chance classification performance (95% threshold) was evaluated by ranking the mean accuracy of the real data within the accuracies obtained from the label shuffled data. Exactly stated, in order to conform to the 95% threshold, the accuracy of the real data had to rank within the 50 highest accuracies of the 1000 label shuffled data.

Furthermore, we analysed the distributions of phase shifts based on each single time-frequency point that was selected to predict subsequent memory pooled across all trials and all subjects. To identify deviations from a uniform distribution Rayleigh tests were performed for each feature and condition. In case of significant Rayleigh tests differences in mean phase shifts between the conditions ‘remembered’ and ‘forgotten’ were tested by Watson–Williams tests (i.e. the circular analogue of the two-sample *t*-test).

## Results

The overall accuracy (27 subjects) of correct classifications into the categories ‘remembered’ and ‘forgotten’ was 64.9% using one rhinal

TABLE 1. Frequencies and time points based on which classification features were chosen in each patient

Pat	Phase shift						Absolute phase					
	Freq RH	Time RH	Freq HI	Time HI	Freq Diff	Time Diff	Freq RH	Time RH	Freq HI	Time HI	Freq Diff	Time Diff
1	17.5	1400	13	1710	41.5	20	9.5	150	27.5	1300	27	1180
2	21	750	31.5	660	48.5	170	28.5	400	48	1050	19	1130
3	18	1190	9	20	36	1720	22.5	730	19.5	40	45.5	1440
4	42	1190	30.5	300	46.5	360	12	390	33.5	1050	41	270
5	50	1230	24.5	20	10	890	5.5	40	35.5	830	10	990
6	18.5	620	0.5	680	30.5	1190	29	1420	16	690	0.5	1040
7	36	140	45.5	1160	46	210	48	1210	45	940	41	170
8	3.5	590	15.5	110	9.5	600	27	1340	3	640	40	1230
9	8.5	590	37	340	45	410	49.5	1000	49.5	1360	0.5	1360
10	45	1860	46.5	400	44.5	320	40	510	24.5	380	10	130
11	0.5	330	22.5	120	22.5	70	0.5	1650	1.5	480	44.5	60
12	18	120	1	1640	49.5	1100	24	100	47	1120	45.5	1360
13	22.5	800	48.5	20	32.5	970	41.5	520	2.5	640	22.5	760
14	15	720	49	650	17	1530	35	580	0.5	1220	13.5	310
15	6	1290	36.5	610	10	280	45	620	34.5	620	29.5	550
16	7.5	130	34	1860	36.5	1460	11.5	890	0.5	1040	23.5	100
17	12.5	10	48	10	7.5	1530	2	580	45.5	980	2	1240
18	9	90	19	480	16.5	20	9	30	40.5	1270	43	1750
19	31	270	46.5	630	20	1090	47	280	24.5	200	29.5	870
20	36	620	48	820	28.5	170	0.5	900	44	360	23	320
21	37	640	17	570	41	320	38.5	1170	6.5	1130	15	1490
22	28.5	980	17.5	190	25	290	33	370	29.5	1780	13	1880
23	30.5	920	24.5	1030	34.5	30	12	1870	10.5	1240	49	1940
24	6.5	330	39	40	36	660	39.5	1650	13.5	1020	23.5	510
25	6	160	49	1860	27	380	45	570	40	1240	46.5	1890
26	32.5	630	37.5	670	35.5	10	49	540	0.5	770	29.5	620
27	35	1000	26	150	31	180	15	540	1.5	950	25	1310

RH, rhinal cortex; HI, hippocampus; diff, rhinal–hippocampal phase difference.

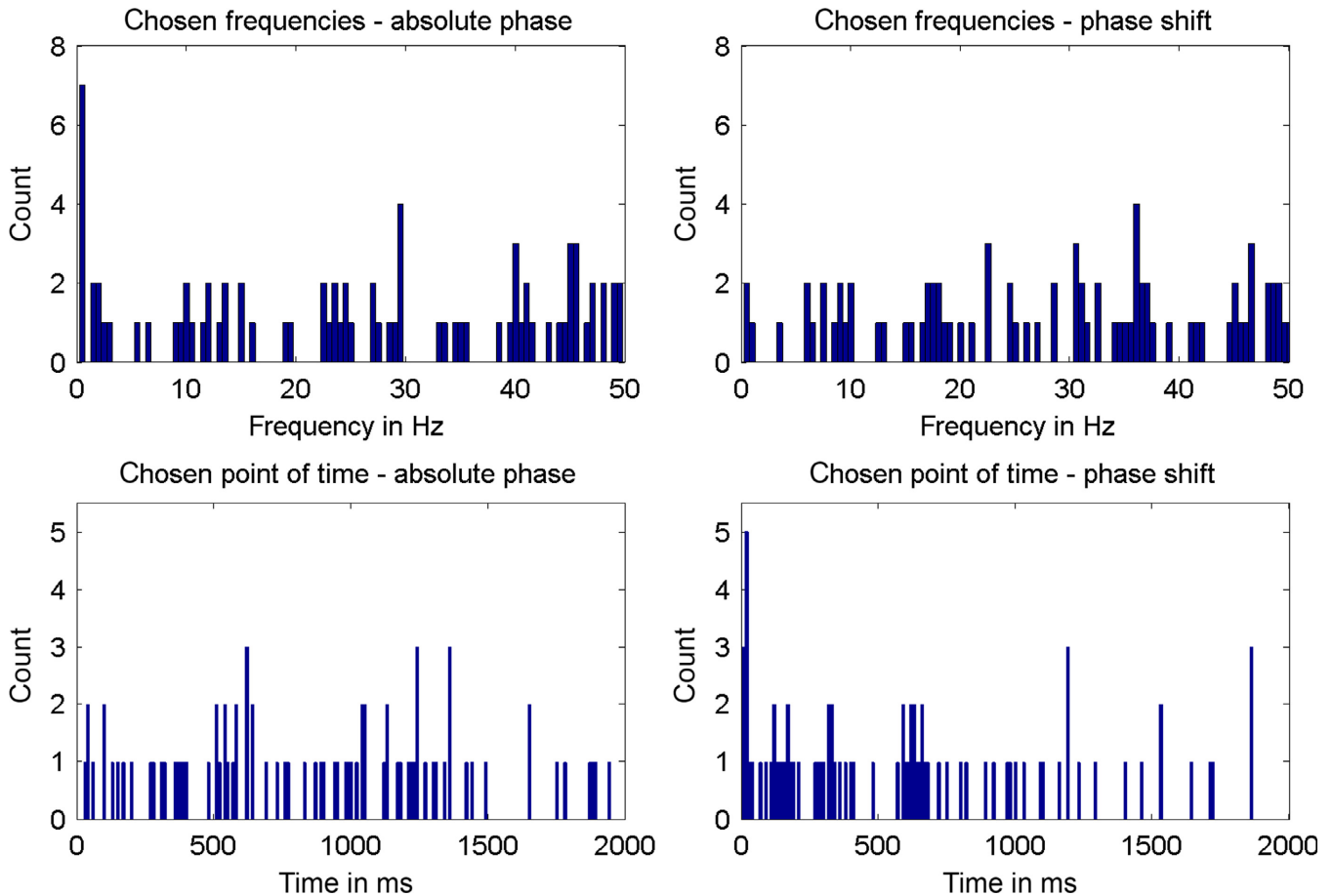


FIG. 2. Distribution of frequencies (top row) and time points (bottom row) chosen as features for classification based on absolute phase values (left column) and phase shifts (right column). The depicted frequencies and time points are pooled over patients and all three features (i.e. hippocampal and rhinal phases and rhinal–hippocampal phase differences, see Table 1). [Colour figure can be viewed at [wileyonlinelibrary.com](http://wileyonlinelibrary.com)].

phase shift value, one hippocampal phase shift value and one rhinal–hippocampal phase difference shift value. Based on label shuffle statistics, results above-chance level were achieved for 19 subjects (Fig. 3A). Using absolute phase values, the overall accuracy was 66.6% and results were above-chance level for 23 subjects.

In addition, we performed classifications based on the inclusion of only one of the three different measures to assess the predictive capability of the individual measures. Based on the prediction accuracies, these measures were ranked. The numerically highest overall classification accuracies were reached based on hippocampal phase values (63.1% for absolute phase vs. 61.2% for phase shift) followed by rhinal–hippocampal phase differences (63.0% for absolute phase difference vs. 60.7% for phase difference shift) and rhinal phase values (62.6% for absolute phase compared to 60.0% for phase shift). Prediction accuracy surpassed chance level in 19 subjects for absolute rhinal phase (vs. nine subjects for rhinal phase shift), in 18 subjects for absolute hippocampal phase (vs. 14 subjects for hippocampal phase shift) and 18 subjects for absolute rhinal–hippocampal phase difference (vs. nine subjects for phase difference shift).

Across subjects, prediction accuracies for classification based on single-trial absolute phases were significantly higher than those based on single-trial phase shifts [two-way repeated measures ANOVA, main effect for MEASURE (absolute phase/phase shift),  $F_{1,75} = 14.38$ ;  $P = 0.0008$ ]. There was no significant difference

between the accuracies for the three different features [no main effect for FEATURE (rhinal cortex/hippocampus/phase difference)  $F_{2,75} = 0.345$ ,  $P = 0.71$ ] and no interaction MEASURE  $\times$  FEATURE ( $F_{2,75} = 0.078$ ,  $P = 0.93$ ) (Fig. 3B).

Combining the three absolute phase-based features chosen from the whole time interval [−500 ms; 2000 ms] used in our previous study (Höhne *et al.*, 2016) and the three poststimulus phase shift-based features, an overall prediction accuracy of 71.1% could be achieved compared to 69.2% for only absolute phase-based features (no significant difference across subjects; paired *t*-test,  $P = 0.14$ ). Thus, classification could not be significantly improved by adding the features based on phase shifts.

Furthermore, we analysed the distributions of phase shifts for the different features and conditions (see Fig. 4). We detected significant deviations from uniform distributions (Rayleigh tests) for rhinal phase shifts in case of remembered trials ( $P = 0.022$ ; mean = −1.12), for shifts of rhinal–hippocampal phase differences in case of remembered ( $P = 1.27\text{e-}16$ ) and forgotten trials ( $P = 2.75\text{e-}28$ ), as well as trends for hippocampal phase shifts in case of both conditions ( $P = 0.056$  and  $P = 0.057$ ). No significant deviation from a uniform distribution was detected for rhinal shifts in case of forgotten trials ( $P = 0.44$ ). Differences between mean phase shifts for remembered and forgotten trials (Watson–Williams test) were significant for the hippocampus ( $P = 0.00048$ ; mean = 1.09 vs. 0.62) indicating larger phase shifts for later

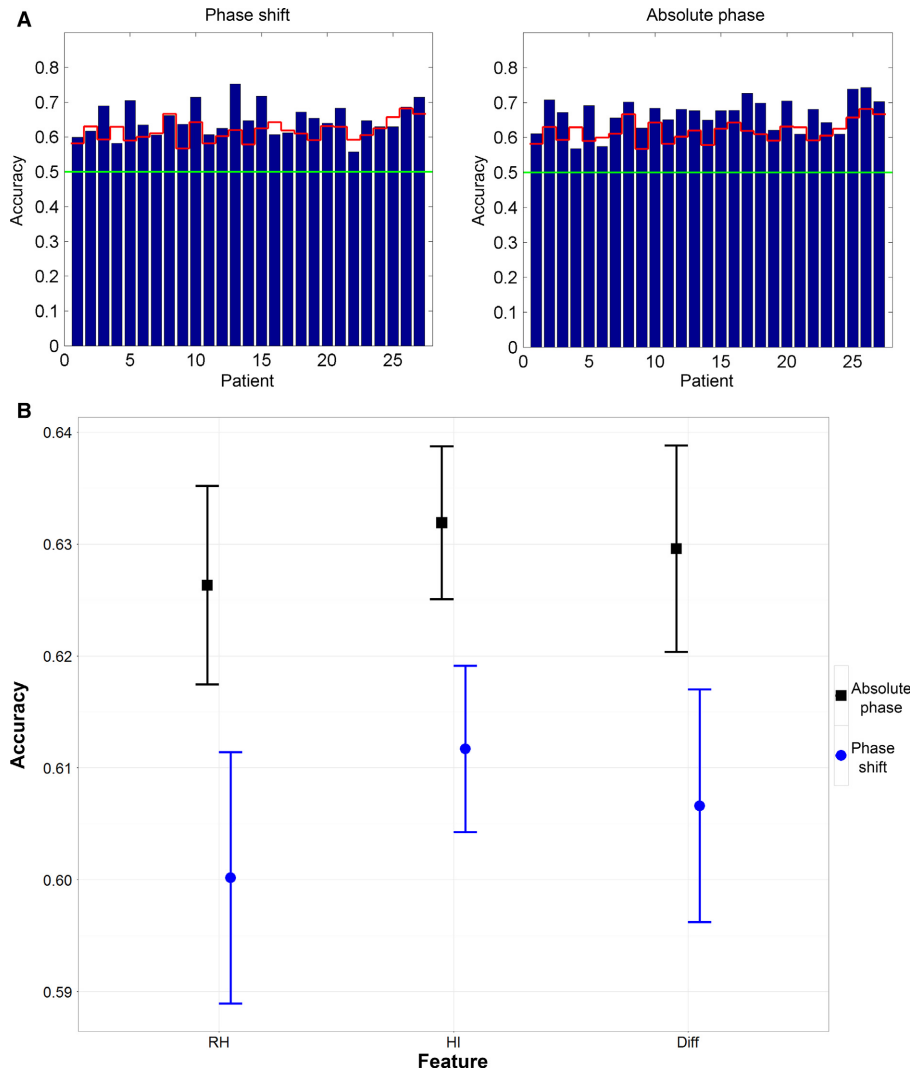


FIG. 3. (A) Prediction accuracies per patient for prediction based on stimulus-related phase shifts (left side) and based on absolute phase values (right side). The upper (red) lines mark the individual 95% threshold based on non-parametric label permutation statistics; the lower straight (green) line marks the 50% accuracy. (B) Prediction accuracies based on single features for absolute phase values (squares) and phase shifts (dots). Mean accuracy across patients and the standard error (SE) are shown here. RH, rhinal cortex; HI, hippocampus; Diff, rhinal–hippocampal phase difference. [Colour figure can be viewed at [wileyonlinelibrary.com](http://wileyonlinelibrary.com)].

remembered items. Mean phase shifts for rhinal–hippocampal phase differences did not significantly differ between conditions ( $P = 0.88$ ; mean = 0.10 vs. 0.09).

Finally, we performed several control analyses. First, we investigated whether our results may be biased by data characteristics, which are unrelated to phase dynamics. For this purpose, we constructed for each patient and each channel so-called phase-scrambled surrogate data that is data with power spectra identical to the original data, but randomly rearranged phases (Theiler *et al.*, 1992). For these surrogate data, we recalculated the prediction analyses including new feature selections. Across patients, the prediction results for the phase-scrambled data were not significantly different from 50% chance level neither for absolute phases (two-tailed  $t$ -test,  $P = 0.72$ ) nor for phase shifts ( $P = 0.85$ ). This indicates that our results are specifically related to rhinal and hippocampal phase dynamics, and are not biased by other data characteristics.

Second, we evaluated whether the prediction results can be mainly attributed to the rhinal N400 and the hippocampal P600 component. For this purpose, we subtracted for each patient the

average ERPs from the individual trials (separately for remembered and forgotten trials) and recalculated prediction accuracies for the previously determined time-frequency points. We found that the newly calculated prediction accuracies did not significantly differ from the previously calculated accuracies across patients neither for absolute phases (paired two-tailed  $t$ -test,  $P = 0.96$ ) nor for phase shifts ( $P = 0.65$ ). This suggests that the reported prediction results are not dominated by effects related to the N400 and P600 component.

Third, we investigated whether individual prediction accuracies depend on signal-to-noise ratios. For this purpose, we calculated the signal-to-noise ratios for each patient based on the absolute values of peak amplitudes of the N400/P600 components divided through the standard deviation of amplitudes across all time points and trials. Pearson's cross-correlations were quantified between individual prediction accuracies based on absolute phases/phase shifts and rhinal/hippocampal signal-to-noise ratios. Indeed, we found statistical trends for positive correlations between prediction accuracies based on absolute phases and rhinal signal-to-noise

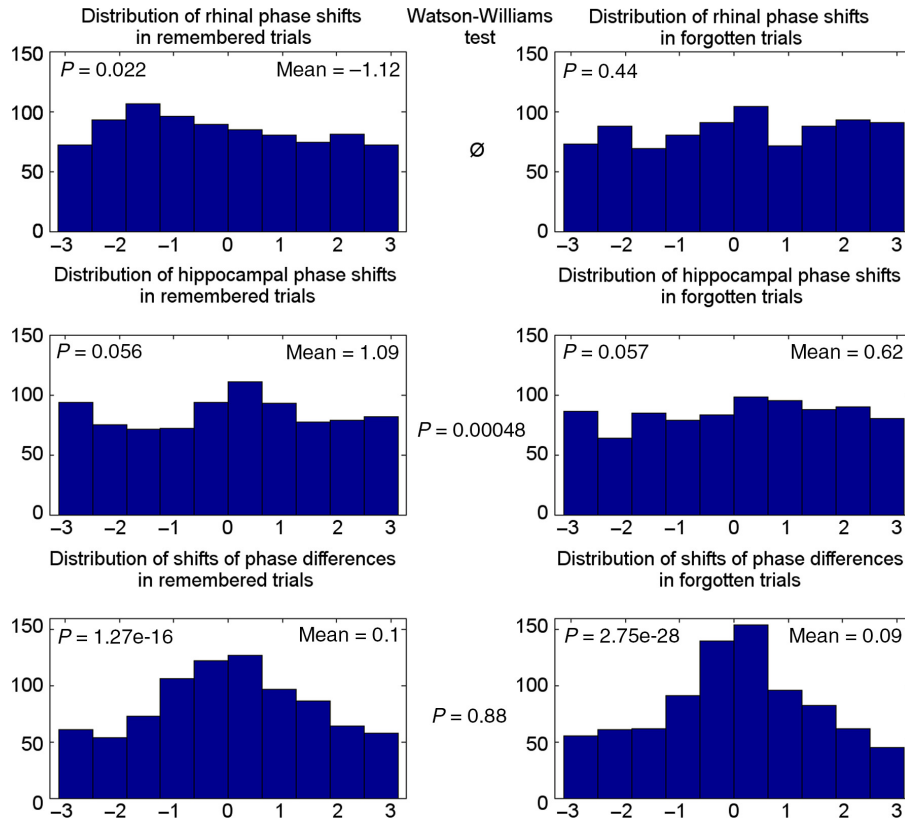


FIG. 4. Distribution of phase shifts for remembered (left column) and forgotten (right column) trials for the three selected features (rhinal cortex, hippocampus and rhinal–hippocampal difference). The  $x$ -axis depicts the values of the phase shifts (radians  $\in [-\pi; \pi]$ , bin width =  $\pi/5$ ), the  $y$ -axis depicts the number of trials exhibiting these phase shifts.  $P$ -values for the Rayleigh tests are depicted in the left upper corner of the histograms and  $P$ -values for the Watson–Williams tests can be found in the centre column. [Colour figure can be viewed at [wileyonlinelibrary.com](http://wileyonlinelibrary.com)].

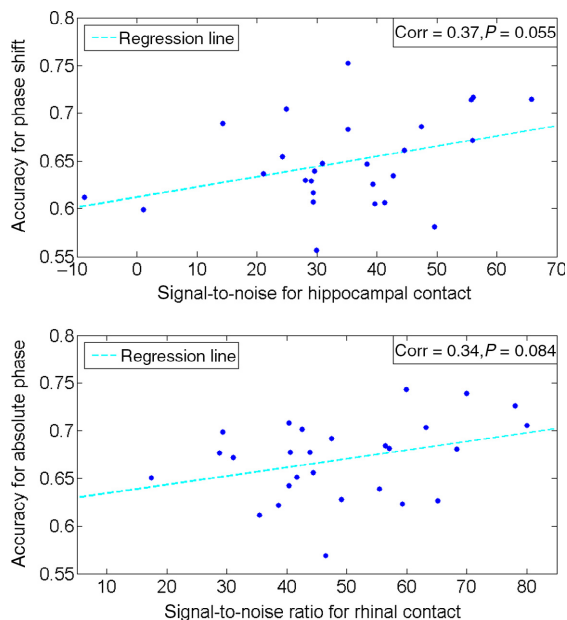


FIG. 5. Prediction accuracies for each patient vs. signal-to-noise-ratios (SNR) for the chosen contacts. Regression lines are plotted in dashed style. Pearson's cross-correlations and related  $P$ -values are depicted in the right upper corner. Top: Prediction accuracies based on phase shifts vs. SNR for hippocampal contacts. Bottom: Prediction accuracies based on absolute phases values vs. SNR for rhinal contacts. [Colour figure can be viewed at [wileyonlinelibrary.com](http://wileyonlinelibrary.com)].

ratios (corr = 0.34,  $P = 0.084$ ), as well as between prediction accuracies based on phase shifts and hippocampal signal-to-noise ratios (corr = 0.37,  $P = 0.055$ ; see Fig. 5). There was no significant correlation between prediction accuracies based on absolute phases and hippocampal signal-to-noise ratios ( $P = 0.81$ ), and between prediction based on phase shifts and rhinal signal-to-noise ratios ( $P = 0.41$ ).

Fourth, we calculated a frequency-resolved prediction analysis for fixed time windows to ascertain whether the major result, that is higher prediction accuracies for absolute phases vs. phase shifts, generalises for this condition. We performed this recalculation for rhinal phases/phase shifts with a fixed time window centred at 400 ms (corresponding to the N400 component) and for hippocampal phases/phase shifts with a fixed time window centred at 600 ms (corresponding to the P600 component) separately for each frequency between 0.5 and 50 Hz. Across patients, prediction accuracies were not different from 50% chance level for the phase shifts for any of the frequencies examined. For the absolute phases, prediction accuracies were above 50% chance level for six frequencies (6.5, 10, 10.5, 19.5, 30, 33 Hz; two-tailed  $t$ -tests each  $P < 0.05$ ). Comparing prediction accuracies for absolute phases vs. phase shifts across patients revealed significantly higher accuracies for the absolute phases (paired two-tailed  $t$ -test,  $P = 0.0064$ ; see Fig. 6), in accordance with the main results of the feature selection-based analysis.

Fifth, we conducted a prediction analysis using a different prediction method consisting of a generalised linear model (GLM). For prediction, we used frequencies in the theta/alpha range (3–12 Hz) and again, a fixed time window centred at 400 ms (corresponding to

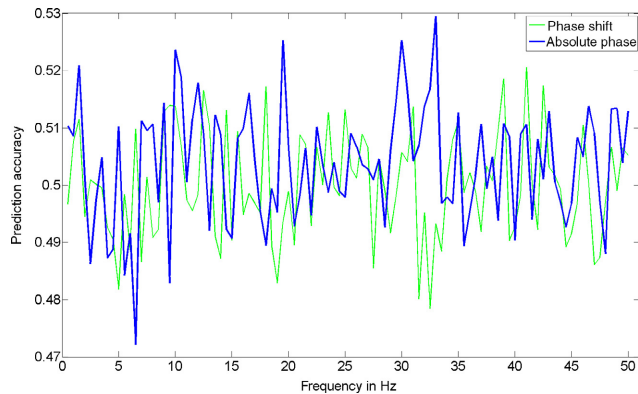


FIG. 6. Frequency-resolved average prediction accuracies across patients based on rhinal and hippocampal absolute phases (bold blue curve) and phase shifts (narrow green curve). Features were selected for each frequency between 0.5 and 50 Hz and fixed time windows centred at 400 ms (corresponding to the N400 component) for rhinal phases/phase shifts and at 600 ms (corresponding to the P600 component) for hippocampal phases/phase shifts. [Colour figure can be viewed at [wileyonlinelibrary.com](http://wileyonlinelibrary.com)].

the N400 component) for rhinal phases/phase shifts and a fixed time window centred at 600 ms (corresponding to the P600 component) for hippocampal phases/phase shifts. The quality of predictions based on absolute phases vs. phase shifts was evaluated by the Akaike information criterion (AIC; Akaike, 1974) and both models were compared by the Vuong-test (Vuong, 1989), which is suitable for comparison of non-nested GLMs. The GLMs based on absolute phases vs. phase shifts yielded AIC values of 4195 vs. 4236 (a lower AIC value indicates a better model). The Vuong-test revealed a significant difference between the quality of both models ( $P = 0.043$ ). When fitting the GLMs to the training data and applying them to the test data, the GLM based on absolute phases yielded an average prediction accuracy of 54.9% and the GLM based on phase shifts revealed an average prediction accuracy of 48.1%. Across patients, prediction accuracies were above 50% chance level for the absolute phases (two-tailed  $t$ -test,  $P = 0.025$ ). For the relative phases, prediction accuracies were not significantly different from 50% chance level ( $P = 0.75$ ). Finally, comparing GLM-based prediction accuracies for absolute phases vs. phase shifts across patients revealed a trend for higher accuracies for the absolute phases (paired two-tailed  $t$ -test,  $P = 0.07$ ).

## Discussion

In a previous study, we found that absolute single-trial phase values are predictive for successful memory formation (Höhne *et al.*, 2016). However, it remained unclear whether the magnitude of rhinal and hippocampal phase shifts as a marker of effective stimulus processing is relevant for memory formation (e.g. Achuthan & Canavier, 2009). In line with this hypothesis, we detected larger mean hippocampal phase shifts and more accumulated rhinal phase shifts for later remembered compared to forgotten trials. But are phase shifts similarly well-suited to predict memory formation as absolute phases? The present data show that absolute phase values clearly outperform stimulus-related phase shifts in terms of predicting memory formation. Moreover, there is no significant improvement of subsequent memory classification when adding phase shift features to the absolute phase values.

Rhinal and hippocampal absolute phases possibly affect memory formation via influencing neural membrane potentials and thereby

controlling firing thresholds (e.g. Elbert & Rockstroh, 1987), that is via a mechanism of spike-field coupling. Such modulations of neural activity by field potential oscillations comparable to those measured *in vivo* have been demonstrated *in vitro* and in simulations (e.g. Anastassiou *et al.*, 2010; Fröhlich & McCormick, 2010). The memory-predictive capability of rhinal and hippocampal absolute phases thus may reflect whether inhibition or facilitation of neural firing occur precisely at the right time point within the required processing sequence or not. Moreover, the absolute phases of low-frequency oscillations have been shown to control the direction of synaptic changes in the hippocampus (Pavlidis *et al.*, 1988; Huerta & Lisman, 1993). Absolute phases depend on the phase values at stimulus presentation and on stimulus-related phase shifts. The present data confirm that the absolute rhinal and hippocampal phases *per se* and not stimulus-related phase shifts are most crucial for successful memory formation.

## Acknowledgements

This study was supported by the German Research Foundation via the collaborative research centre SFB 1089. We would like to thank Eva Ludowig for her contributions to data acquisition and preprocessing.

## Conflict of interest

None of the authors has a financial interest or a potential conflict of interest to declare.

## Data accessibility

Data supporting the results can be made available upon request.

## Author contributions

M.D. and J.F. designed the study. M.D. analysed the data. M.D., A.J., C.B., N.A. and J.F. wrote the manuscript.

## Abbreviations

EEG, electroencephalography; iEEG, intracranial EEG; LTM, long-term memory; SVM, support vector machine.

## References

- Achuthan, S. & Canavier, C.C. (2009) Phase-resetting curves determine synchronization, phase locking and clustering in networks of neural oscillators. *J. Neurosci.*, **29**, 5218–5233.
- Akaike, H. (1974) A new look at the statistical model identification. *IEEE Trans. Autom. Control*, **19**, 716–723.
- Anastassiou, C.A., Montgomery, S.M., Barahona, M., Buzsáki, G. & Koch, C. (2010) The effect of spatially inhomogeneous extracellular electric fields on neurons. *J. Neurosci.*, **30**, 1925–1936.
- Berens, P. (2009) CircStat: a MATLAB toolbox for circular statistics. *J. Stat. Softw.*, **31**, 1–21.
- Burke, J.F., Long, N.M., Zaghoul, K.A., Sharan, A.D., Sperling, M.R. & Kahana, M.J. (2014) Human intracranial high-frequency activity maps episodic memory formation in space and time. *NeuroImage*, **85**, 834–843.
- Duvernoy, H.M. (1988). *The Human Hippocampus. An Atlas of Applied Anatomy*. J.F. Bergmann Verlag, München, pp. 25–43.
- Elbert, T. & Rockstroh, B. (1987) Threshold regulation – a key to the understanding of the combined dynamics of EEG and event-related potentials. *J. Psychophysiol.*, **1**, 317–333.
- Fell, J. & Axmacher, N. (2011) The role of phase synchronization in memory processes. *Nat. Rev. Neurosci.*, **12**, 105–118.
- Fell, J., Ludowig, E., Rosburg, T., Axmacher, N. & Elger, C.E. (2008) Phase-locking within human mediotemporal lobe predicts memory formation. *NeuroImage*, **43**, 410–419.

- Fröhlich, F. & McCormick, D.A. (2010) Endogenous electric fields may guide neocortical network activity. *Neuron*, **67**, 129–143.
- Höhne, M., Jahanbekam, A., Bauckhage, C., Axmacher, N. & Fell, J. (2016) Prediction of successful memory encoding based on single-trial rhinal and hippocampal phase information. *NeuroImage*, **139**, 127–135.
- Huerta, P.T. & Lisman, J.E. (1993) Heightened synaptic plasticity of hippocampal CA1 neurons during a cholinergically induced rhythmic state. *Nature*, **364**, 723–725.
- Lopour, B.A., Tavassoli, A., Fried, I. & Ringach, D.L. (2013) Coding of information in the alpha phase of local field potentials within human medial temporal lobe. *Neuron*, **79**, 594–606.
- Ludowig, E., Trautner, P., Kurthen, M., Schaller, C., Bien, C.G., Elger, C.E. & Rosburg, T. (2008) Intracranially recorded memory-related potentials reveal higher posterior than anterior hippocampal involvement in verbal encoding and retrieval. *J. Cogn. Neurosci.*, **20**, 841–851.
- Maris, E. & Oostenveld, R. (2007) Nonparametric statistical testing of EEG- and MEG-data. *J. Neurosci. Meth.*, **164**, 177–190.
- Oostenveld, R., Fries, P., Maris, E. & Schoffelen, J.-M. (2011) FieldTrip: open source software for advanced analysis of MEG, EEG, and invasive electrophysiological data. *Comput. Intell. Neurosci.*, **2011**, 156869.
- Pavlidis, C., Greenstein, Y.J., Grudman, M. & Winson, J. (1988) Long-term potentiation in the dentate gyrus is induced preferentially on the positive phase of theta-rhythm. *Brain Res.*, **439**, 383–387.
- Sederberg, P.B., Schulze-Bonhage, A., Madsen, J.R., Bromfield, E.B., McCarthy, D.C., Brandt, A., Tully, M.S. & Kahana, M.J. (2007) Hippocampal and neocortical gamma oscillations predict memory formation in humans. *Cereb. Cortex*, **17**, 1190–1196.
- Theiler, J., Eubank, S., Longtin, A., Galdrikian, B. & Farmer, J.D. (1992) Testing for nonlinearity in time series: the method of surrogate data. *Physica D*, **58**, 77–94.
- Vuong, Q.H. (1989) Likelihood ratio tests for model selection and non-nested hypotheses. *Econometrica*, **57**, 307–333.
- Womelsdorf, T., Schoffelen, J.M., Oostenveld, R., Singer, W., Desimone, R., Engel, A.K. & Fries, P. (2007) Modulation of neuronal interactions through neuronal synchronization. *Science*, **316**, 1609–1612.